A structural, theoretical and coordinative evaluation of the bicyclic guanidinate derived from 1,4,6-triazabicyclo[3.3.0]oct-4-ene

Majid S. Khalaf, Martyn P. Coles* and Peter B. Hitchcock

Received 16th April 2008, Accepted 16th May 2008
First published as an Advance Article on the web 17th June 2008
DOI: 10.1039/b806510a

Partial deprotonation of the bicyclic guanidine 1,4,6-triazabicyclo[3.3.0]oct-4-ene (Htbo) is achieved using ^{n}BuLi. Isolation of the resulting lithium salts has resulted in the structural characterization of the mixed anion complex $\{[Li(tbo)(\mathbf{VIII})(tboH)]_2\}_\infty$ **1a** (where **VIII**-H = 1-(2-aminoethyl)-2-imidazolidinethione) and the partially deprotonated salt $Li_6(tbo)_6(Htbo)_3$, **1b**. The neutral guanidine Htbo reacts cleanly with $AlMe_3$ and $ZnMe_2$ to afford the organometallic complexes $[Al(tbo)Me_2]_2$ [**2**]$_2$, and $Zn_3(tbo)_4Me_2$ (**3**). Structural characterization of these compounds enables comparison between the {5:5}-bicyclic system, [tbo]$^-$, and the previously reported {6:6}-bicyclic system, [hpp]$^-$ (where hppH = 1,3,4,6,7,8-hexahydro-2*H*-pyrimido[1,2-*a*]pyrimidine). Results indicate that delocalization within the [tbo]$^-$ anion is restricted to the CN_2 amidinate component, with retention of electron density in the non-bonding nitrogen lone-pair. These conclusions are supported by a DFT analysis of the neutral guanidines, Htbo and hppH.

Introduction

Amidinates, $[RC\{NR'\}_2]^-$ (**I**, Fig. 1), and their amido-substituted guanidinate counterparts, $[R_2NC\{NR'\}_2]^-$ (**II**, Fig. 1), continue to evolve as versatile *N*,*N*′-donor groups in coordination chemistry.[1] Their flexibility in this role is largely due to the range of derivatives accessible through substitution at the nitrogen positions, enabling them to serve as ligands to metals from across the periodic table. Many bonding modes have been observed for both classes of ligand including chelation to a single metal, affording a four-membered metallacycle, and bridging two-, three- or even four-metals in the construction of multi-metallic clusters.

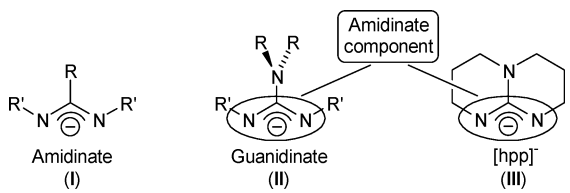

Fig. 1 General formulae for amidinate, guanidinate and the [hpp]$^-$ anions.

A specific class of guanidinate ligand that displays diverse coordination behaviour is based on the bicyclic guanidine, 1,3,4,6,7,8-hexahydro-2*H*-pyrimido[1,2-*a*]pyrimidine (hppH).[2] The anion derived from this neutral compound, [hpp]$^-$ (**III**, Fig. 1), exhibits significant differences in both its steric and electronic properties when compared with that derived from its acyclic relatives **II**. For example, the ligand has a propensity to bridge rather than bind a single metal (although chelation has been observed in a number of complexes[3–5]), a feature that was extensively exploited by Cotton and co-workers in the development of bimetallic 'paddle-wheel' compounds.[6] This is attributed to the parallel projection of the two *N*-donor orbitals (**IV**, Fig. 2) contrasting to the convergence of these orbitals at the 'mouth' of the ligand in the acyclic derivatives (**V**, Fig. 2).[7] [hpp]$^-$ has also been described as 'electron-rich' due to the accessibility of the zwitterionic resonance form **VI** (Fig. 2) arising from delocalization of the lone-pair of the non-bonding nitrogen atom into the CN_2 amidinate component of the ligand.[4,5] Both of these features arise from the constraints imposed by the bicyclic system, effectively pulling the nitrogen substituents away from the ligand aperture (**IV**) and enforcing the correct orbital alignment to promote π-delocalization in the CN_3 core of the ligand (**VI**).

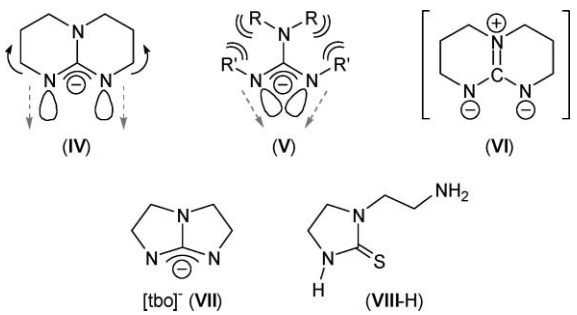

Fig. 2 Abbreviations and key bonding features referred to in this work.

Recent publications by Cotton and co-workers have extended the family of bicyclic guanidines to include those which contain fused {5:5}-, {5:6}-[8] and {7:5}-, {7:6}-[9] ring systems, as well as those incorporating additional alkyl-substituents.[10] To date, work has focused on the application of these ligand precursors in the synthesis of new paddle-wheel complexes, although a recent report has been presented in which the anion derived from 1,4,6-triazabicyclo[3.3.0]oct-4-ene (Htbo) was used as an ancillary ligand in gold(I) chemistry.[11] Our interests lie in the more general application of ligands of this type in coordination chemistry,[12] and as such we report here our early findings on the [tbo]$^-$ anion

Department of Chemistry, University of Sussex, Falmer, Brighton, BN1 9QJ, UK; Fax: +44 (0)1273 677196; Tel: +44 (0)1273 877339

(**VII**, Fig. 2) as a ligand at Li, Al and Zn, enabling structural comparisons to be made with their $[hpp]^-$ analogues.

Experimental

General experimental procedures

All manipulations were carried out under dry nitrogen using standard Schlenk line and cannula techniques, or in a conventional nitrogen-filled glovebox operating at <1 ppm oxygen. Solvents were dried over the appropriate drying agent and degassed prior to use. The reagents $AlMe_3$ (2.0 M solution in hexanes) and $ZnMe_2$ (2.0 M solution in toluene) were purchased from commercial sources and used as received. The compound Htbo was made according to literature procedures.[8] NMR spectra were recorded using a Bruker Avance DPX 300 MHz spectrometer at 300 (^{1}H) and 75 ($^{13}C\{^1H\}$) MHz, or a Varian VNMRS 400 MHz spectrometer at 400 (^{1}H) and 100 ($^{13}C\{^1H\}$) MHz. Proton and carbon chemical shifts were referenced internally to residual solvent resonances. Elemental analyses were performed by S. Boyer at London Metropolitan University.

Synthetic procedures

General procedure for the reaction of Htbo with ^{n}BuLi. A sample of the neutral guanidine, Htbo, was dissolved in THF and cooled to −78 °C. ^{n}BuLi (0.5–1.0 equivalents of a 1.6 M solution in hexanes) was added *via* syringe and the reaction allowed to warm to room temperature. The solution was filtered to remove any particulate material and crystal growth was attempted under various conditions.

Isolation of 1a. A small quantity of crystals suitable for X-ray analysis were isolated from a reaction between ^{n}BuLi and Htbo contaminated with the monocyclic compound, 1-(2-aminoethyl)-2-imidazolidinethione (**VIII**-H). No further analysis was obtained on this product.†

Isolation of 1b. 0.25 g Htbo (2.25 mmol) was dissolved in Et_2O and cooled to −78 °C. 1.4 mL ^{n}BuLi (1.6 M solution in hexanes, 2.25 mmol) was added by syringe and the mixture was allowed to warm to room temperature and was stirred for 15 h. The resultant cloudy solution was filtered and stored at room temperature, affording colourless crystals suitable for X-ray diffraction.† Yield 0.12 g, 46% (based on Htbo). Anal. calc. for $C_{45}H_{75}Li_6N_{27}$: C 52.17, H 7.30, N 36.51%. Found: C 52.09, H 7.28, N 36.41%.

Synthesis of $[Al(tbo)Me_2]_2$ [2]$_2$. 1.12 mL of a hexane solution of $AlMe_3$ (2.0 M, 2.25 mmol) was added dropwise to a slurry of Htbo (0.25 g, 2.25 mmol) in Et_2O at −78 °C. The mixture was allowed to warm to room temperature and was stirred under ambient conditions for 15 h. The solution was filtered and maintained at room temperature, affording small colourless crystals of **2**.† Yield 0.26 g, 68%. Anal. calc. for $C_7H_{14}AlN_3$: C 50.29, H 8.44, N 25.13%. Found: C 50.18, H 8.58, N 24.98%. ^{1}H NMR (300 MHz, 303 K, C_6D_6): δ 3.58 (pseudo t, 4H, tbo-CH_2), 2.28 (pseudo t, 4H, tbo-CH_2), −0.26 (s, 6H, AlMe_2). ^{13}C NMR (100 MHz, 303 K, C_6D_6): δ 176.1 (CN_3), 54.6, 47.8 (tbo-CH_2), −8.1 (AlMe_2). Mass Spec (EI^+, m/z) 319 ([**2**]$_2$ − Me)$^+$.

Synthesis of $Zn_3(tbo)_4Me_2$ 3. 1.80 mL of a toluene solution of $ZnMe_2$ (2.0 M, 3.60 mmol) was added dropwise to a solution of Htbo (0.40 g, 3.60 mmol) in toluene at −78 °C. The mixture was allowed to warm to room temperature and was stirred under ambient conditions for 18 h, affording a cloudy solution. Heating (~80 °C) and filtering gave a clear solution that was allowed to cool slowly to room temperature, affording colourless crystals suitable for X-ray analysis.† Yield 0.39 g, 65% (based on Htbo). Anal. calc. for $C_{22}H_{38}N_{12}Zn_3$: C 39.63, H 5.74, N 25.21%. Found: C 39.72, H 5.79, N 25.19%. ^{1}H NMR (400 MHz, 303 K, C_6D_6): δ 3.82 (m, 4H, tbo-CH_2), 3.73 (m, 12H, tbo-CH_2), 2.71 (m, 16H, tbo-CH_2), −0.39 (s, 6H, ZnMe_2). ^{13}C NMR (100 MHz, 303 K, C_6D_6): δ 182.2 (br, CN_3), 178.5 (CN_3), 55.8, 55.7, 50.8, 48.8 (tbo-CH_2), 1.5 (ZnMe_2).

Crystallographic details

Details of the crystal data, intensity collection and refinement for complexes **1a**, **1b**, [**2**]$_2$ and **3** are collected in Table 1. Crystals were covered in an inert oil and suitable single crystals were selected under a microscope and mounted on a Kappa CCD diffractometer. The structures were refined with SHELXL-97.[13] Additional features of note:

$Li_6(tbo)_6(Htbo)_3$ 1b. N24 is disordered over two resolved positions. The H atoms on N21, N23, and N26 were refined; others were in riding mode.

$[Al(tbo)Me_2]_2$ [2]$_2$. The lower occupancy site for the disordered N6 atom was left isotropic.

$Zn_3(tbo)_4Me_2$ 3. The identified toluene solvate molecules were included with isotropic C atoms. Additional void space is noted within the structure; however, given that the maximum residual electron density is ~0.5 e Å^{-3}, inclusion of additional solvent molecules in these voids was not deemed sensible.

Results and discussion

Complexes of lithium

The most widely used protocol for attaching a guanidinate anion to a metal is *via* salt metathesis involving the corresponding lithium reagent. Frequently, this route does not involve isolation of the lithium species, which is generated and reacted *in situ* through the addition of an alkyl lithium reagent to the neutral guanidine in a donor solvent. However, as we were interested in examining the bonding within the guanidinate using X-ray crystallography, initial work focused on attempting to isolate and crystallize the lithium salt of the $[tbo]^-$ anion.

Whilst the fully deprotonated species $[Li(tbo)(solvent)_x]_n$, has not yet been isolated and characterized, crystallographic analysis of the products from these reactions has revealed some interesting structural features and are discussed in the following section. We note, however, that the solution-state structures are difficult to ascertain due to low solubility of the aggregated species and high lattice energies leading to problems in re-dissolving the isolated crystalline products.

† CCDC reference numbers 685440–685443. For crystallographic data in CIF or other electronic format see DOI: 10.1039/b806510a

Table 1 Crystal structure and refinement data for **1a**, **1b**, $[\mathbf{2}]_2$ and **3**

	1a	**1b**	$[\mathbf{2}]_2$	**3**
Formula	$C_{15}H_{27}Li_2N_9S{\cdot}C_4H_8O$	$C_{45}H_{75}Li_6N_{27}{\cdot}C_4H_{10}O$	$C_{14}H_{28}Al_2N_6$	$C_{22}H_{38}N_{12}Zn_3{\cdot}2(C_7H_8)$
Formula weight	451.50	1110.08	334.38	851.02
Temperature/K	173(2)	173(2)	173(2)	173(2)
Wavelength/Å	0.71073	0.71073	0.71073	0.71073
Crystal size/mm	0.25 × 0.20 × 0.15	0.40 × 0.40 × 0.30	0.40 × 0.40 × 0.30	0.20 × 0.20 × 0.10
Crystal system	Triclinic	Triclinic	Triclinic	Tetragonal
Space group	$P\bar{1}$ (No.2)	$P\bar{1}$ (No.2)	$P\bar{1}$ (No.2)	$I\bar{4}$ (No.82)
a/Å	10.1795(3)	14.2908(2)	8.5214(2)	20.5807(8)
b/Å	10.4390(3)	15.0897(2)	10.1796(3)	20.5807(8)
c/Å	12.4108(4)	15.2485(2)	12.2236(2)	20.3647(9)
α/°	78.589(2)	68.643(1)	99.825(2)	90
β/°	67.596(2)	79.395(1)	103.853(2)	90
γ/°	83.120(2)	88.720(1)	114.523(1)	90
V/Å^3	1193.74(6)	3006.54(7)	891.79(4)	8625.8(6)
Z	2	2	2	8
D_c/Mg m^{-3}	1.26	1.23	1.25	1.31
Absorption coefficient/mm^{-1}	0.17	0.08	0.17	1.69
θ range for data collection/°	3.45 to 26.04	3.42 to 26.04	3.64 to 26.05	3.44 to 25.99
Reflections collected	17634	47304	13658	19504
Independent reflections	4665 [$R_{int} = 0.044$]	11783 [$R_{int} = 0.036$]	3495 [$R_{int} = 0.033$]	8306 [$R_{int} = 0.054$]
Reflections with $I > 2\sigma(I)$	3780	9459	3242	6048
Data/restraints/parameters	4665/0/301	11783/0/770	3495/0/208	8306/0/392
Goodness-of-fit on F^2	1.032	1.018	1.059	1.055
Final R indices [$I > 2\sigma(I)$]	$R_1 = 0.047$, $wR_2 = 0.113$	$R_1 = 0.057$, $wR_2 = 0.137$	$R_1 = 0.036$, $wR_2 = 0.096$	$R_1 = 0.065$, $wR_2 = 0.151$
R indices (all data)	$R_1 = 0.063$, $wR_2 = 0.123$	$R_1 = 0.073$, $wR_2 = 0.148$	$R_1 = 0.039$, $wR_2 = 0.098$	$R_1 = 0.101$, $wR_2 = 0.169$
Largest diff. peak/hole/e Å^{-3}	0.31 and −0.40	0.56 and −0.59	0.24 and −0.29	0.53 and −0.50

The first complex to be studied resulted from the lithiation of a batch of Htbo contaminated with the intermediate monocyclic species 1-(2-aminoethyl)-2-imidazolidinethione (**VIII**-H, Fig. 2), which apparently co-sublimes with the desired product.[14] As expected, **VIII**-H also reacts with ^{n}BuLi to form the corresponding imidazolinethionate anion, and the resulting product generated from this mixture (**1a**), was shown to contain a 1 : 1 ratio of both the [tbo]$^-$ and [**VIII**]$^-$ anions.

The molecular structure of **1a** (Fig. 3, Table 2) is composed of a symmetry related $[Li_2(tbo)(\mathbf{VIII})]_2$ dimer, in which the [tbo]$^-$ anions are bonded in a $\kappa^{1,2}N$–$\kappa^{3,4}N'$-mode above and below the Li_4-plane (Fig. 4). The resultant Li_2N_2-metallacycles are non-planar (fold angle at nitrogen = 160.3 °) with acute internal angles at nitrogen [78.24(13)° and 78.07(13)° at N1 and N2, respectively] compared with lithium [102.07(14)° and 98.83(14)° at Li1 and Li2, respectively]. The two eclipsed Li_2N_2 groups form a roughly cubic unit that is bridged across opposite Li···Li edges by a [**VIII**]$^-$ anion in a $\kappa^{1,2}N$-bridging mode, with Li–N distances of 2.101(3) Å and 2.121(3) Å to Li1 and Li2, respectively. The distorted tetrahedral geometry of each lithium is completed by either an N_{imine}-bound neutral Htbo ligand (Li1), which hydrogen bonds to sulfur [H5x···S = 2.52 Å], or by an –NH_2 group from the [**VIII**]$^-$ anion of a neighbouring Li_4N_4-unit (Li2). The latter 'inter-unit' bonding links the molecules into a one dimensional

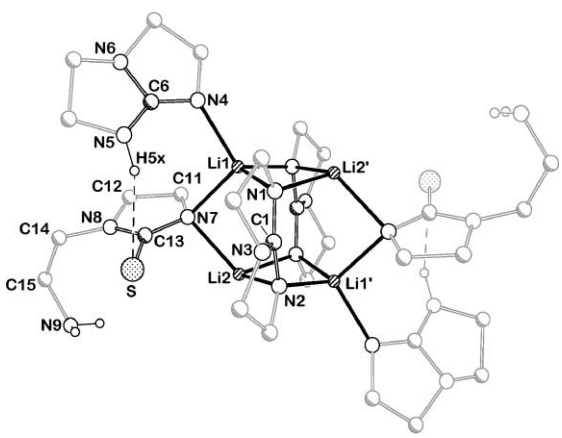

Fig. 3 Molecular structure of the dimeric $[Li_2(tbo)(\mathbf{VIII})(Htbo)]_2$ unit of **1a**. Hydrogen atoms, except N*H* of Htbo and NH_2 of [**VIII**]$^-$, are omitted.

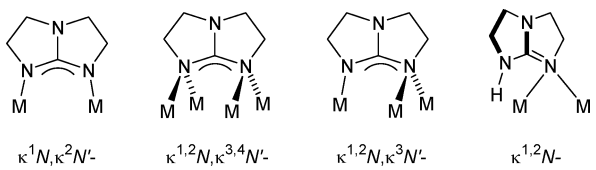

Fig. 4 Bonding modes for the [tbo]$^-$ and Htbo ligands encountered during this work.

Table 2 Selected bond lengths (Å) for **1a**

Li1–N1	2.050(3)	Li2–N2	2.103(4)
Li1–N7	2.101(3)	Li2–N7	2.121(3)
Li1–N4	2.040(3)	Li1–N2′	2.054(3)
Li2–N1′	2.099(4)	Li2–N9″	2.068(4)
C1–N1	1.323(2)	C1–N2	1.330(2)
C1–N3	1.407(2)	C6–N4	1.286(3)
C6–N5	1.344(3)	C6–N6	1.381(2)
N7–C11	1.482(2)	N7–C13	1.316(2)
N8–C12	1.435(3)	N8–C13	1.371(2)
C11–C12	1.514(3)	C13–S	1.7217(18)

Symmetry equivalent atoms: $' = -x + 1, -y + 1, -z + 1$; $'' = -x + 1, -y, -z + 1$.

chain *via* macrocyclic $[(C_3N_2S)CH_2CH_2NH_2Li]_2$ structures, with short Li2–N9″ bonds of 2.068(4) Å, (Fig. 5).

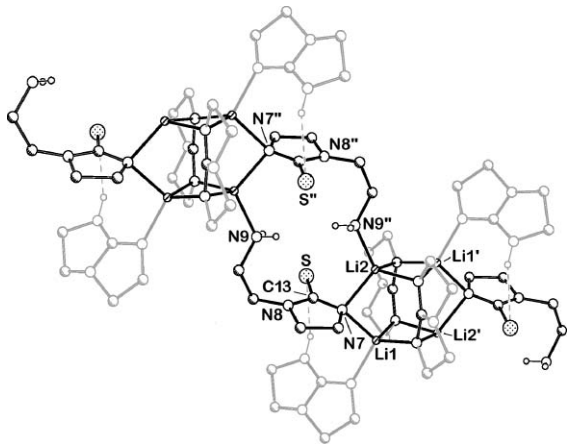

Fig. 5 A segment of the chain structure of compound **1a**.

The face-capping coordination of the [tbo]$^-$ anion to four lithium atoms is similar to that observed for [hpp]$^-$ in cubic-based frameworks of lithium atoms.[15,16] The nitrogen–lithium distances in **1a** [2.050(3) Å to 2.103(4) Å] are unexceptional and lie within the range observed for the [hpp]$^-$ anion in a similar bonding arrangement. The bond lengths within the imidazolidinethione anion is not significantly perturbed from that in the neutral species,[8] although a slight increase in the carbon–sulfur distance is noted in the anionic form (**1a**, 1.7217(18) Å; **VIII**-H, 1.687(2) Å).

The presence of both [tbo]$^-$ and Htbo as ligands in **1a** enables detailed examination of the bonding (parameters defined in Fig. 6) using criteria previously used to help explain the distribution of electron density within charged and neutral forms of guanidines.[4,17] As expected, the carbon–nitrogen bonds within the amidine component of the neutral Htbo are more localized than in the anion, shown clearly by the greater value for Δ_{CN} (Htbo, 0.058 Å; [tbo]$^-$, 0.007 Å). Further examination of carbon–nitrogen distances shows that in contrast to the π-delocalization typically observed throughout the CN_3 core of the [hpp]$^-$ anion, the distance from the central carbon to the non-bonding nitrogen in [tbo]$^-$ is relatively long [1.407(2) Å], resulting in a large Δ'_{CN} value of 0.081 Å. This observation is consistent with a retention of electron-density at N3, and is reinforced by the high degree of pyramidalization (DP = 29.1%) at this atom. To put these figures into context, the corresponding values for fourteen independent examples of the [hpp]$^-$ anion with the same $\kappa^{1,2}N$–$\kappa^{3,4}N'$-bonding mode in lithium clusters gave a range of Δ'_{CN} from 0.008 Å to 0.065 Å, and a maximum DP value of 1.7%.[15,16]

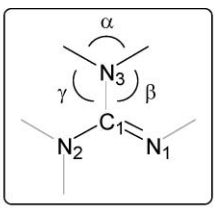

$$\Delta_{CN} / Å = (C_1–N_2) - (C_1–N_1)$$

$$\Delta'_{CN} / Å = (C_1–N_3) - [\{(C_1–N_1) + (C_1–N_2)\} / 2]$$

$$DP\ \% = [360 - (\alpha + \beta + \gamma)] / 0.9$$

Fig. 6 Geometric parameters used to describe the bonding in neutral and anionic guanidine-based ligands.

Lithiation of a pure sample of Htbo using 1.0 equivalents of ^{n}BuLi, and allowing the reaction to stir for 15 h at room temperature, afforded colourless crystals suitable for analysis by X-ray diffraction (**1b**). The structure showed that under these conditions, deprotonation is incomplete, affording the mixed guanidinate:guanidine salt, $Li_6(tbo)_6(Htbo)_3$. This compound bears resemblance to the partially deprotonated pyridylaniline, [Ph(2-pyr)NLi]·(HMPA)·[Ph(2-pyr)NH],[18] and the more recently reported salt $[Li(hpp)(hppH)]_2$,[16] although the guanidinate:guanidine ratio in **1b** is 2 : 1, rather than 1 : 1 observed for hppH. Spectroscopic analysis of **1b** was hampered by the low solubility of the product, precluding the acquisition of meaningful NMR data. However, bulk purity was indicated from elemental analysis results, indicating that **1b** was the major product from this reaction.

The molecular structure of **1b** is shown in Fig. 7 and selected bond lengths and angles in Table 3. Atoms Li1-Li4 are incorporated in a Li_4N_4-cluster with two $\kappa^{1,2}N$–$\kappa^{3,4}N'$-bonding guanidinates, forming a common basic structural unit to that found in **1a**. The additional two lithium atoms are held in position by bridging κ^1N–κ^2N'-bound [tbo]$^-$ anions at distances of 3.19 Å and 3.06 Å, and the resultant Li1–Li2–Li5–Li6 plane is capped by an additional $\kappa^{1,2}N$–$\kappa^{3,4}N'$-guanidinate. The final [tbo]$^-$ anion terminates this folded ladder arrangement of lithium atoms, being κ^1N–κ^2N'-bound to Li5 and Li6. The three neutral Htbo ligands are located at Li3 and Li4, with each metal bound by a terminal guanidine and a $\kappa^{1,2}N$-bridge. These neutral ligands are further secured by hydrogen bonds in the range 2.86–2.96 Å between the N*H* and either a nitrogen from the amidinate component of a bridging [tbo]$^-$ anion (N7 and N16) or to the non-bonding nitrogen of a capping ligand (N3).

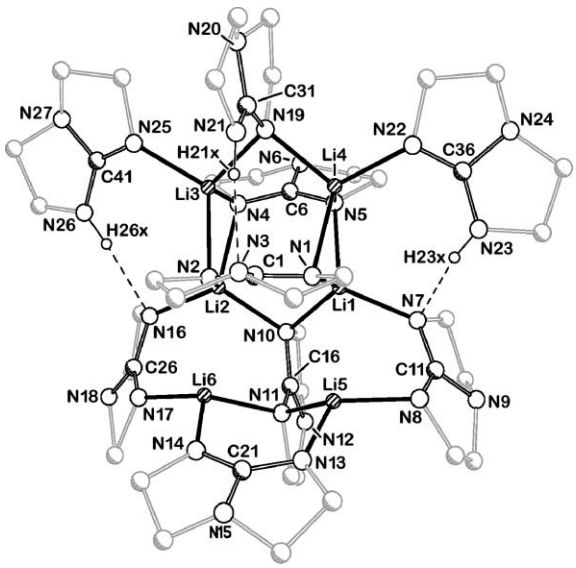

Fig. 7 Molecular structure of $Li_6(tbo)_6(Htbo)_3$. Hydrogen atoms, except N*H* of Htbo, and ether solvate are omitted.

The overall arrangement of lithium atoms in **1b** is therefore best described as two intersecting Li_4-planes, with a fold angle of

Table 3 Selected bond lengths (Å) for **1b**

Li1–N1	2.100(3)	Li2–N2	2.108(3)
Li1–N5	2.122(3)	Li2–N4	2.114(3)
Li1–N7	2.010(3)	Li2–N16	2.036(3)
Li1–N10	2.063(4)	Li2–N10	2.035(3)
Li3–N2	2.183(3)	Li4–N1	2.179(3)
Li3–N4	2.043(3)	Li4–N5	2.042(3)
Li3–N19	2.118(3)	Li4–N19	2.056(3)
Li3–N25	2.020(3)	Li4–N22	2.023(3)
Li5–N8	2.002(4)	Li6–N17	1.987(4)
Li5–N11	2.049(4)	Li6–N11	2.032(4)
Li5–N13	1.994(4)	Li6–N14	1.971(4)
C1–N1	1.324(2)	C1–N2	1.329(2)
C1–N3	1.410(2)	C6–N4	1.325(2)
C6–N5	1.327(2)	C6–N6	1.405(2)
C11–N7	1.330(2)	C11–N8	1.312(2)
C11–N9	1.409(2)	C16–N10	1.321(2)
C16–N11	1.316(2)	C16–N12	1.400(2)
C21–N13	1.321(2)	C21–N14	1.321(2)
C21–N15	1.415(2)	C26–N16	1.328(3)
C26–N17	1.311(2)	C26–N18	1.415(2)
C31–N19	1.308(2)	C31–N20	1.370(2)
C31–N21	1.337(2)	C36–N22	1.276(3)
C36–N23	1.342(3)	C36–N24	1.438(4)
C41–N25	1.291(3)	C41–N26	1.340(3)
C41–N27	1.388(3)		

68.81° at Li1 and Li2 (Fig. 8). This is somewhat unusual given the propensity for lithium guanidinate species to aggregate into three dimensional structures,[15,16] although in the majority of these cases, an interstitial ion is present, the structural importance of which is unknown. The guanidinate centred at C1 effectively blocks the lithium atoms wrapping around to form a more compact cluster and, although long to be considered a 'true bond' (N1 ··· Li5 and N2 ··· Li6 distances = 2.76 Å and 2.62 Å, respectively) there is likely to be an electrostatic interaction between these atoms.

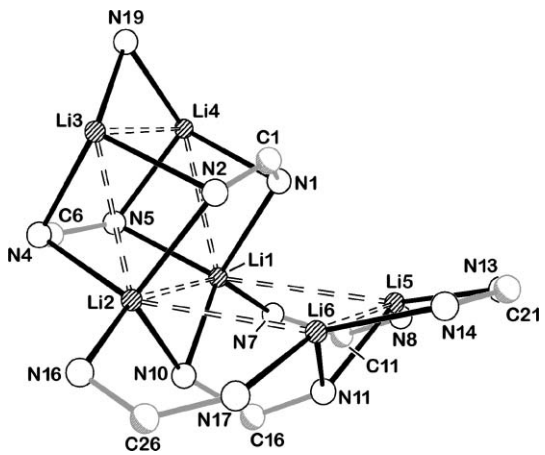

Fig. 8 Li_6-core arrangement in **1b**.

Examining the bonding parameters for the guanidinate component of **1b** (Table 4), we again note relatively large Δ'_{CN} values (range 0.079–0.096 Å) with predominantly pyramidal non-bonding nitrogen atoms. The relatively low DP value of 8.3% for N12 is due to the ligand being effectively sandwiched between two additional guanidinates, forcing the substituents into the plane of the nitrogen atom. This sterically induced configuration does not, however, appear to promote delocalization of the lone-pair into the CN_3 core to any great extent, as the Δ'_{CN} value is unexceptional for this class of anion.

Table 4 Summary of bonding parameters within the [tbo]$^-$ and Htbo ligands of **1b**

Atoms	Bonding type	Δ_{CN}/Å	Δ'_{CN}/Å	DP
C1 N1–3	$\kappa^{1,2}N$–$\kappa^{3,4}N'$–	0.005	0.084	N3: 26.8%
C6 N4–6	$\kappa^{1,2}N$–$\kappa^{3,4}N'$–	0.002	0.079	N6: 25.7%
C11 N7–9	$\kappa^{1}N$–$\kappa^{2}N'$–	0.018	0.088	N9: 29.6%
C16 N10–12	$\kappa^{1,2}N$–$\kappa^{3,4}N'$–	0.005	0.082	N12: 8.3%
C21 N13–15	$\kappa^{1}N$–$\kappa^{2}N$–′	0	0.094	N15: 29.3%
C26 N16–18	$\kappa^{1}N$–$\kappa^{2}N'$–	0.017	0.096	N18: 30.8%
C31 N19–21[a]	$\kappa^{1,2}N$–	0.062	—	N20: 20.6%
C36 N22–24[a,b]	$\kappa^{1}N$–	0.066	—	—
C41 N25–27[a]	$\kappa^{1}N$–	0.049	—	N27: 24.9%

[a] Neutral Htbo ligand; [b] N24 disordered over two positions, precluding DP measurments.

Complexes of aluminium and zinc

Previous work has shown that hppH reacts cleanly with one equivalent of $AlMe_3$[7] or $ZnMe_2$[19] *via* protonolysis of the organometallic bond and elimination of methane. With aluminium, the expected Al(hpp)Me_2 (**A**) product is formed and crystallographic analysis shows a bridging κ^1N–κ^2N'-mode for the guanidinate in a dimeric complex containing an eight-membered '$Al_2C_2N_4$' metallacycle. In the corresponding reaction with zinc, the trimetallic compound $Zn_3(hpp)_4Me_2$ (**B**) is formed in which both κ^1N–κ^2N'- and $\kappa^{1,2}N$–κ^3N'-bridging modes are observed for the guanidinate.

The reaction between $AlMe_3$ and Htbo at room temperature yields colourless crystals that analyze as the mono-guanidinate complex, Al(tbo)Me_2, **2**. The ^{1}H and ^{13}C NMR spectra show two resonances for the annular methylene groups of the guanidinate ligand and a single high field resonance for the AlMe_2 groups, consistent with a symmetric species in solution. The EI-mass spectrum shows a highest mass peak at 319 amu, corresponding $[Al_2(tbo)_2Me]^+$ formed by loss of a methyl group from the dimer. X-Ray crystallographic analysis confirms that $[\mathbf{2}]_2$ is dimeric in the solid-state (Fig. 9, Table 5).

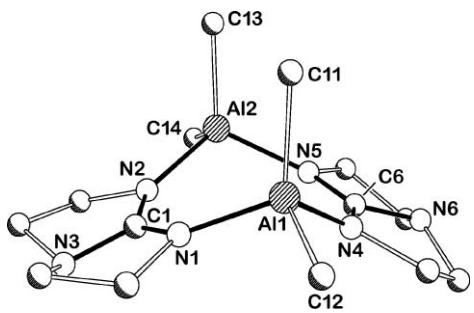

Fig. 9 Molecular structure of [Al(tbo)Me_2]$_2$ $[\mathbf{2}]_2$ with hydrogen atoms omitted.

As for the [hpp]$^-$ analogue, the guanidinate ligand bridges two aluminium centres to generate an eight-membered metallacycle. In contrast to **A**, however, a 'boat-like' conformation is present in $[\mathbf{2}]_2$ rather than the less sterically congested 'chair' in [Al(hpp)Me_2]$_2$, indicating that the [tbo]$^-$ anion imposes significantly different geometrical constraints when complexed to a metal. Spectroscopic

Table 5 Selected bond lengths (Å) and angles (°) for $[\mathbf{2}]_2$

Al1–N1	1.9026(14)	Al2–N2	1.9084(13)
Al1–N4	1.9143(15)	Al2–N5	1.9166(13)
Al1–C11	1.9605(17)	Al2–C13	1.9644(17)
Al1–C12	1.9790(18)	Al2–C14	1.9747(17)
C1–N1	1.329(2)	C6–N4	1.326(2)
C1–N2	1.3244(19)	C6–N5	1.326(2)
C1–N3	1.3837(19)	C6–N6	1.403(3)
N1–Al1–N4	108.04(6)	N2–Al2–N5	109.86(6)
N1–Al1–C11	112.88(7)	N2–Al2–C13	110.83(7)
N1–Al1–C12	104.76(8)	N2–Al2–C14	105.10(7)
N4–Al1–C11	110.85(7)	N5–Al2–C13	113.62(7)
N4–Al1–C12	104.92(8)	N5–Al2–C14	103.40(7)
C1–N3–C4	106.64(12)	C6–N6–C9	108.09(15)
C1–N3–C3	106.34(13)	C6–N6–C8	104.9(2)
C3–N3–C4	124.81(13)	C8–N6–C9	128.65(19)

data indicate that this conformation is not rigid in solution as time averaged signals are noted for the different methyl environments in both the ^{1}H and ^{13}C NMR spectra. Cooling a sample to −40 °C does not resolve the different methyl environments, indicating a low barrier to inter-conversion. We feel that this is most likely explained by a rapid chair-to-boat conformational change, although rupture and reformation of the metallacycle cannot be ruled out.

As expected, the Δ_{CN} values for the [tbo]$^-$ anions are negligible, consistent with delocalization across the amidinate component. The Δ'_{CN} value for the non-disordered ligand of $[\mathbf{2}]_2$ (0.06 Å) is considerably larger than in **A** (0.01 Å), with N3 exhibiting a much greater pyramidalization (DP = 24.7%) than the corresponding non-bonding nitrogen of the [hpp]$^-$ (DP = 0%). It may be expected that the increased electron density at the bonding nitrogen atoms in [hpp]$^-$ (resonance form **VII**) would be manifest in shorter Al–N distances in **A**. However, this electronic effect is offset by a reduced steric bulk of the [tbo]$^-$ ligand due to the smaller rings in the bicyclic framework, resulting in insignificant differences in the average Al–N distances.

The stoichiometric reaction between Htbo and $ZnMe_2$ in toluene afforded colourless crystals on work-up that analyzed as the trimetallic complex, $Zn_3(tbo)_3Me_2$ (**3**). The NMR spectra indicate a non-fluxional system with two distinct environments for the guanidinate ligand, later confirmed by X-ray diffraction analysis.

The molecular structure of **3** is analogous to that formed from the reaction between hppH and $ZnMe_2$ (**B**),[19] comprised of a trigonal planar array of three zinc atoms (Fig. 10, Table 6). Each of the metals has a distorted tetrahedral geometry; two of the zinc centres (Zn2 and Zn3) retain a methyl substituent with the third (Zn1) bound only by nitrogen. The guanidinates centred about C1 and C6 bridge zinc in a κ^1N,κ^2N'-coordination, the remaining two anions centered at C11 and C16 present in a $\kappa^{1,2}N,\kappa^3N'$-coordination to three metals. Despite similarities in the structures of **3** and **B**, the inter-metal distance supported by the [tbo]$^-$ ligand is significantly greater than in the [hpp]$^-$ analogue (Fig. 11). This can be explained in simple geometric terms by the angle between the outward projecting orbitals being greater for two fused pentagons *versus* two hexagons,[8] and represents another significant difference in the bonding displayed by these two similar guanidinates.

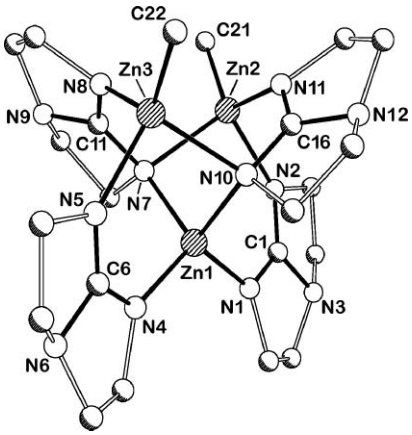

Fig. 10 Molecular structure of $Zn_3(tbo)_4Me_2$ (**3**). Hydrogen atoms and toluene solvate molecules are omitted.

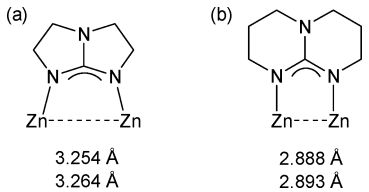

Fig. 11 Crystallographically determined zinc···zinc distances for $Zn_3(L)_4Me_2$ (a) L = [tbo]$^-$, **3**; (b) L = [hpp]$^-$, **B**.

Table 6 Selected bond lengths (Å) and angles (°) for **3**

Zn1–N1	1.963(6)	Zn1–N4	1.956(6)
Zn1–N7	2.027(6)	Zn1–N10	2.056(7)
Zn2–N2	2.006(6)	Zn2–N7	2.204(6)
Zn2–N11	2.019(6)	Zn3–N5	2.025(8)
Zn3–N8	2.009(7)	Zn3–N10	2.193(6)
Zn2–C21	1.972(8)	Zn3–C22	1.969(10)
C1–N1	1.336(10)	C1–N2	1.314(10)
C1–N3	1.406(10)	C6–N4	1.324(11)
C6–N5	1.310(12)	C6–N6	1.390(11)
C11–N7	1.381(9)	C11–N8	1.297(10)
C11–N9	1.373(9)	C16–N10	1.345(10)
C16–N11	1.305(10)	C16–N12	1.376(10)
N1–Zn1–N4	117.6(3)	N4–Zn1–N7	116.5(3)
N1–Zn1–N7	102.2(3)	N4–Zn1–N10	101.6(3)
N1–Zn1–N10	117.0(3)	N7–Zn1–N10	101.3(2)
C21–Zn2–N2	116.4(4)	C21–Zn2–N11	120.0(4)
C21–Zn2–N7	116.9(3)	N2–Zn2–N11	103.4(3)
N2–Zn2–N7	95.7(2)	N7–Zn2–N11	100.7(2)
C22–Zn3–N8	122.2(4)	C22–Zn3–N5	114.4(4)
C22–Zn3–N10	114.7(4)	N5–Zn3–N8	104.6(3)
N8–Zn3–N10	101.7(2)	N5–Zn3–N10	95.2(3)
C1–N3–C3	107.4(6)	C1–N3–C4	103.4(6)
C3–N3–C4	127.3(8)	C6–N6–C8	105.5(7)
C6–N6–C9	104.2(8)	C8–N6–C9	127.5(8)
C11–N9–C13	108.1(6)	C11–N9–C14	105.4(6)
C13–N9–C14	129.2(7)	C16–N12–C18	106.7(6)
C16–N12–C19	104.3(6)	C18–N12–C19	130.3(6)

DFT analysis

The electronic structures of neutral hppH (**C**) and Htbo (**D**) have been examined using the B3LYP density functional theory and the 6-31g(d) basis set, implemented by the Gaussian 03 suite of programs.[20] Geometry optimizations were performed using the coordinates from X-ray data as a starting point, and defining the C=N and C–N components of the amidine unit as double

Table 7 Summary of key geometric parameters from the calculated structures of hppH (**C**) and Htbo (**D**)

	hppH (**C**)	Htbo (**D**)
C=N/Å	1.290	1.281
C–N/Å	1.394	1.380
Δ_{CN}/Å	0.104	0.099
DP[a]	1.3%	22.0%

[a] Value for the tertiary amino nitrogen.

and single bonds, respectively.‡ The calculated values of Δ_{CN} are displayed in Table 7 and are in agreement with those predicted for neutral, localized systems. The DP values reflect those observed in the solid-state (*vide supra*), with a much larger value for the Htbo guanidine reflecting a non-planar amino nitrogen atom. Natural bond orbital analysis (Gaussian NBO Version 3.1) of **C** and **D** reveal some interesting differences in the electronic structures of the two neutral compounds. Initially, examining the natural atomic charges of the N-atoms (Fig. 12), we see a significantly higher negative charge for the imine nitrogen of hppH (−0.658) compared with the same atom of Htbo (−0.591), indicating a greater electron density at this atom. Comparing the orbital contributions from which the nitrogen lone-pairs are comprised (Table 8) the N_{imine} lone-pairs in each case approximate to sp^2-hybrids with a slightly greater *p*-contribution in hppH. The major difference, however, is in the non-bonding (N_2) tertiary amino lone-pair, which is effectively a *p*-orbital for hppH but contains about 13% *s*-character for Htbo (reflected in the HOMO, Fig. 12).

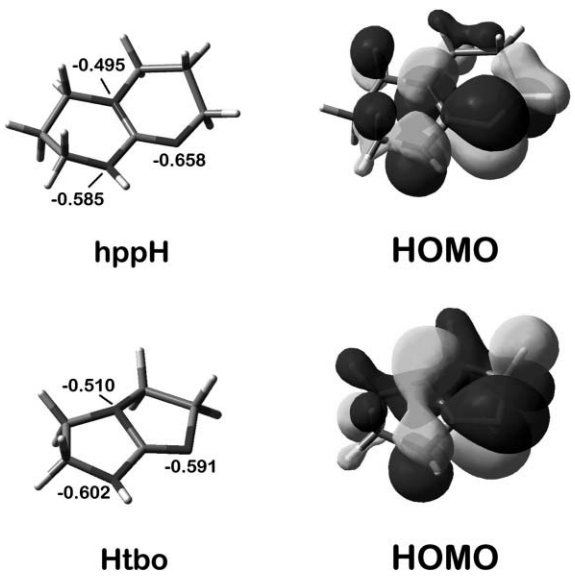

Fig. 12 Optimized structures showing the NPA charges and highest occupied molecular orbitals for hppH (**C**) and Htbo (**D**).

Second order perturbation theory analysis allows an estimation of the stabilization arising from delocalization within the two molecules. In **C** we note a stabilization of 15.14 kcal mol^{-1} arising from delocalization of the N_1 lone-pair into the C–N_2 anti-bonding orbital, with the corresponding value for **D** calculated as 12.13 kcal mol^{-1}. Greater stabilization arises from N_2 and N_3 lone-pair delocalization into the C–N_1 anti-bond, with almost equal contribution for each overlap in **C** (55.76 kcal mol^{-1} and 57.44 kcal mol^{-1}, respectively). In **D**, however, the stabilization derived from the lone-pair on N2 is much reduced (28.82 kcal mol^{-1}), commensurate with increased localization of the lone-pair at this position.

‡ Disorder and the formation of hydrogen-bonded dimers in the crystal structure of hppH rendered the original carbon–nitrogen distances of the amidine component unreliable.

Table 8 Percentage contribution of *s*- and *p*-character to the lone-pair orbitals of the nitrogen atoms in hppH (**C**) and Htbo (**D**)

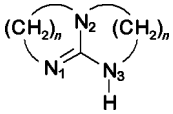

	hppH (**C**)		Htbo (**D**)	
Atom	*s*-	*p*-	*s*-	*p*-
N_1	31.99%	67.94%	37.45%	62.42%
N_2	0.04%	99.95%	12.79%	87.14%
N_3	0.17%	99.82%	0%	100%

The HOMO for both **C** and **D** are similar in appearance, with the Htbo orbital stabilized by ~8.2 kcal mol^{-1} relative to its hppH counterpart. In both cases, the electron density associated with the imine nitrogen extends into the C=N double bond, which is in turn anti-bonding with respect to delocalization across the remainder of the CN_3 core. This lobe of the HOMO also forms the 'donor-orbital' component of these ligands, where in Htbo it extends further suggesting a better neutral donor behaviour. The contribution to the HOMO from the *p*-orbital of the tertiary amino-nitrogen is distorted for Htbo due to the pyramidalization at this atom and overlap with the corresponding *p*-orbital of the secondary amino nitrogen.

Conclusions

We have shown that the [tbo]$^-$ anion is an effective ligand at lithium, aluminium and zinc centres, with bridging between metals a preferred coordination mode in each case. In contrast to hppH where full deprotonation is rapidly accomplished using ^{n}BuLi, the corresponding reaction with Htbo does not appear to go to completion under mild reaction conditions, forming an unusual extended array of six lithium atoms in the mixed guanidinate:guanidine complex, $Li_6(tbo)_6(Htbo)_3$ (**1b**). This indicates that an alternative strategy may be more appropriate for generation of the lithium salt of the {5:5}-fused ring system for further reactivity *via* a salt metathesis protocol. Protonolysis and alkane elimination from aluminium and zinc methyls, however, does proceed cleanly to the expected products.

Examination of the structural parameters of the [tbo]$^-$ guanidinate in the metal complexes reported in this study clearly demonstrates retention of electron density at the non-bonding nitrogen atom, as shown by the large values of Δ'_{CN} and the degree of pyramidalization at this atom. DFT calculations of the neutral hppH and Htbo guanidines, in particular NBO analysis, are in agreement with this hypothesis. Although these observations suggest that a weaker metal–nitrogen bond will result due to a decreased contribution from the zwitterionic resonance **VI**, this appears to be compensated for by the reduced bulk of the [tbo]$^-$

anion arising from the smaller {5:5}-bicyclic framework, enabling the ligand to approach more closely to the highly electropositive metals used in this study.

Other structural differences are, however, noted between the compounds formed with $[tbo]^-$ and their $[hpp]^-$ analogues. For the dimeric aluminium compound $[Al(tbo)Me_2]_2$ **[2]**$_2$, the different conformation of the metallacycle ('boat' for $[tbo]^-$; 'chair' for $[hpp]^-$) is likely to result from small differences in energy arising from crystal packing forces, as spectroscopic measurements indicate that this spatial arrangement is not maintained in solution. For the trimetallic zinc complex $Zn_3(tbo)_4Me_2$ **3**, the significant increase in the inter-metallic Zn···Zn distance compared with $Zn_3(hpp)_3Me_2$ **B** illustrates a general feature of this ligand and how it bridges metal centres. We anticipate that this will be important in the further development of coordination compounds incorporating this anion, particularly given the propensity of bicyclic guanidinates to form aggregated metal clusters.

Notes and references

1 J. Barker and M. Kilner, *Coord. Chem. Rev.*, 1994, **133**, 219; F. T. Edelmann, *Coord. Chem. Rev.*, 1994, **137**, 403; P. J. Bailey and S. Pace, *Coord. Chem. Rev.*, 2001, **214**, 91.

2 This compound is also known as 1,5,7-triazabicyclo[4.4.0]dec-5-ene, and commonly abbreviated as tbdH.

3 F. A. Cotton, J. P. Donahue, N. E. Gruhn, D. L. Lichtenberger, C. A. Murillo, D. J. Timmons, L. O. van Dorn, D. Villagran and X. Wang, *Inorg. Chem.*, 2006, **45**, 201; D. B. Soria, J. Grundy, M. P. Coles and P. B. Hitchcock, *J. Organomet. Chem.*, 2005, **690**, 2278; M. P. Coles and P. B. Hitchcock, *Inorg. Chim. Acta*, 2004, **357**, 4350; D. B. Soria, J. Grundy, M. P. Coles and P. B. Hitchcock, *Polyhedron*, 2003, **22**, 2731; S. R. Foley, G. P. A. Yap and D. S. Richeson, *Polyhedron*, 2002, **21**, 619; F. A. Cotton, C. A. Murillo and X. Wang, *Inorg. Chim. Acta*, 2000, **300**, 1.

4 M. P. Coles and P. B. Hitchcock, *Organometallics*, 2003, **22**, 5201.

5 M. P. Coles and P. B. Hitchcock, *J. Chem. Soc., Dalton Trans.*, 2001, 1169.

6 *Multiple Bonds between Metal Atoms*, ed. F. A. Cotton, C. A. Murillo and R. A. Walton, Springer Science and Business Media Inc., New York, 2005.

7 S. L. Aeilts, M. P. Coles, D. C. Swenson, R. F. Jordan and V. G. Young, Jr., *Organometallics*, 1998, **17**, 3265.

8 F. A. Cotton, C. A. Murillo, X. Wang and C. C. Wilkinson, *Inorg. Chem.*, 2006, **45**, 5493.

9 F. A. Cotton, C. A. Murillo, X. Wang and C. C. Wilkinson, *Dalton Trans.*, 2006, 4623.

10 F. A. Cotton, C. A. Murillo, X. Wang and C. C. Wilkinson, *Dalton Trans.*, 2007, 3943.

11 A. A. Mohamed, A. P. Mayer, H. E. Abdou, M. D. Irwin, L. M. Pérez and J. P. Fackler, Jr., *Inorg. Chem.*, 2007, **46**, 11165.

12 M. P. Coles, *Dalton Trans.*, 2006, 985.

13 G. M. Sheldrick, *SHELXL-97, Program for the Refinement of Crystal Structures*, Göttingen, 1997.

14 The reaction mixture must be maintained at temperatures above 160 °C for 10 days to ensure that the second cyclization that converts 11-(12-aminoethyl)-12-imidazolidinethione (**VIII**-H) to Htbo takes place.

15 S. R. Boss, M. P. Coles, R. Haigh, P. B. Hitchcock, R. Snaith and A. E. H. Wheatley, *Angew. Chem., Int. Ed.*, 2003, **42**, 5593; S. R. Boss, M. P. Coles, V. Eyre-Brook, F. Garcia, R. Haigh, P. B. Hitchcock, M. McPartlin, J. V. Morey and H. Naka, *Dalton Trans.*, 2006, 5574.

16 M. P. Coles and P. B. Hitchcock, *Chem. Commun.*, 2005, 3165.

17 Z. B. Maksic and B. Kovacevic, *J. Chem. Soc., Perkin Trans. 2*, 1999, 2623.

18 D. Barr, W. Clegg, R. E. Mulvey and R. Snaith, *J. Chem. Soc., Chem. Commun.*, 1984, 469.

19 S. J. Birch, S. R. Boss, S. C. Cole, M. P. Coles, R. Haigh, P. B. Hitchcock and A. E. H. Wheatley, *Dalton Trans.*, 2004, 3568.

20 M. J. Frisch , G. W. Trucks, H. B. Schlegel, G. E. Scuseria, M. A. Robb, J. R. Cheeseman, J. A. Montgomery, Jr., T. Vreven, K. N. Kudin, J. C. Burant, J. M. Millam, S. S. Iyengar, J. Tomasi, V. Barone, B. Mennucci, M. Cossi, G. Scalmani, N. Rega, G. A. Petersson, H. Nakatsuji, M. Hada, M. Ehara, K. Toyota, R. Fukuda, J. Hasegawa, M. Ishida, T. Nakajima, Y. Honda, O. Kitao, H. Nakai, M. Klene, X. Li, J. E. Knox, H. P. Hratchian, J. B. Cross, V. Bakken, C. Adamo, J. Jaramillo, R. Gomperts, R. E. Stratmann, O. Yazyev, A. J. Austin, R. Cammi, C. Pomelli, J. W. Ochterski, P. Y. Ayala, K. Morokuma, G. A. Voth, P. Salvador, J. J. Dannenberg, V. G. Zakrzewski, S. Dapprich, A. D. Daniels, M. C. Strain, O. Farkas, D. K. Malick, A. D. Rabuck, K. Raghavachari, J. B. Foresman, J. V. Ortiz, Q. Cui, A. G. Baboul, S. Clifford, J. Cioslowski, B. B. Stefanov, G. Liu, A. Liashenko, P. Piskorz, I. Komaromi, R. L. Martin, D. J. Fox, T. Keith, M. A. Al-Laham, C. Y. Peng, A. Nanayakkara, M. Challacombe, P. M. W. Gill, B. Johnson, W. Chen, M. W. Wong, C. Gonzalez and J. A. Pople, *Gaussian 03, Revision C.02*, Wallingford, CT, 2004.